ACS APPLIED MATERIALS & INTERFACES

Letter

www.acsami.org

# Silver Thin Film as a Temporal Template and Dopant Source for Vertically Aligned p−n homojunction of ZnO Nanorods

Ji-Hyeon Park,[†,‡] Tae Il Lee,[†,§] Sung-Hwan Hwang,[‡] and Jae-Min Myoung*[,‡]

[‡]Department of Materials Science and Engineering, Yonsei University, 134 Shinchon-dong, Seodaemoon-gu, Seoul, Korea

[§]Department of BioNano Technology and Gachon BioNano Research Institute, Gachon University, Seongnam, Korea

Supporting Information

**ABSTRACT:** A silver thin film is introduced as a temporal template and dopant source for vertically aligned p−n homojunction of ZnO nanorods. The growth of Ag-doped ZnO nanorods was observed over time and the doping effect was determined through various characterization methods. Furthermore, a p−n homojunction diode of ZnO nanorods was fabricated.

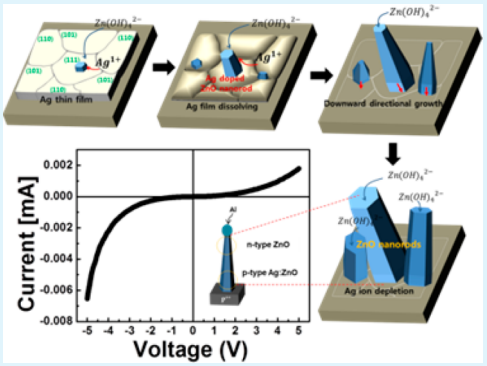


**KEYWORDS:** *Ag-doped ZnO nanorods, Ag thin film, hydrothermal process, template, p−n junction*

## INTRODUCTION

Ever since vertically aligned zinc oxide (ZnO) nanorods (NRs) grown on a substrate using low-temperature hydrothermal processes[1] were shown to be a low-cost and mass-producible n-type semiconducting nanomaterial for electronics, ZnO NRs have been applied as the active semiconducting component in various electronic devices such as light emitting diodes,[2] ultraviolet sensors,[3] gas sensors,[4] nanogenerators,[5] solar cells,[6] and so on. The growth conditions for ZnO NRs have been developed to obtain high performance in each application.[7] However, two essential issues still remain to be solved in the growth of ZnO NRs on a substrate: controlling growth initiation and achieving p-type semiconducting properties.

To be integrated in electronic devices, vertically aligned ZnO NRs should be grown on an electrode. ZnO NRs do not easily grow densely on typical electrodes, with the exception of metal-doped ZnO grown in a conventional low-temperature hydrothermal synthesis using hexamethylenediamine (HMTA). Therefore, a homogeneous seed layer formed by either spin-coating a ZnO sol−gel solution or sputtering ZnO has commonly been used to initiate the growth of ZnO NRs on an electrode substrate.[8] Although the ZnO NRs can be successfully grown on a substrate coated with seed material, crystallographic defects in the seed layer cause an increase in the electrical junction resistance, which degrades the carrier-transport performance from the electrode to the NRs in a device. To overcome this issue, we introduced a sacrificial template, a cobalt hydroxide nanoplate, in our previous work for the growth of ZnO NRs that form an electrical contact with an electrode on a substrate.[9] After conceiving the concept of a sacrificial template, we present here a process to simultaneously achieve p-type doping and growth initiation of ZnO NRs. The principle idea in our process is based on the fact that a thin film template can be dissolved into a solution to be ions and the dissolved ions can then contribute to the doping of p-type ZnO NRs. In this work, we selected a Ag thin film as a temporal template and dopant source for vertically aligned p-type ZnO NRs because Ag can be dissolved in high pH aqueous solutions and is also a p-type doping element in ZnO crystals.[10]

Figure 1(a) depicts the four steps in the growth of ZnO NRs on an Ag thin film template. In the first step, a small seed crystal of ZnO NRs is grown on the (111)-oriented grain of the polycrystalline Ag film, which is continuously dissolved at the highly energetic grain boundaries. In the next step, valleys are formed along the grain boundaries as shown in the schematic diagram, and the ZnO NRs are doped by dissolved $Ag^+$ ions during growth. Additional seed crystals are grown on several (111)-oriented sites that are exposed on the slope of the valleys. The Ag−doped ZnO NRs continue growth until the Ag film completely dissolves, as shown in the third step. As the bottom of the Ag layer supporting the ZnO NRs is gradually dissolved, the NRs extend further downward until finally reaching the substrate. In the final step, after depleting $Ag^+$ ions in the hydrothermal solution, we obtain a p−n homojunction of ZnO NRs through further growth of n-type ZnO NRs. The cross-sectional schematic in this step represents the p−n

Received: July 14, 2014
Accepted: September 5, 2014
Published: September 5, 2014

  

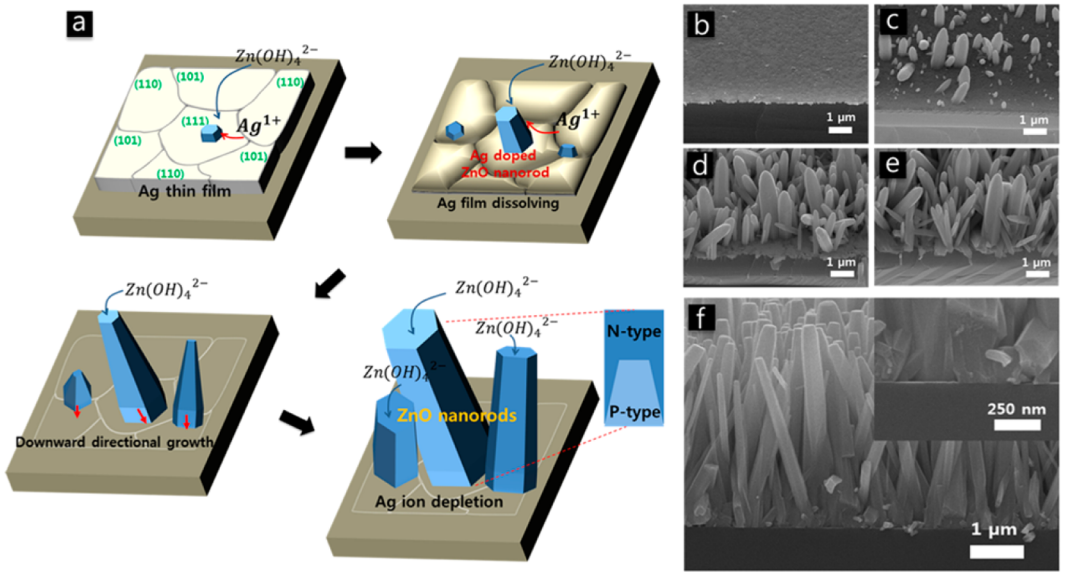


**Figure 1.** (a) Four steps describing the growth of ZnO NRs on a Ag template. Temporal growth of ZnO NRs on a Ag thin film after (b) 30, (c) 45, (d) 60, (e) 75, and (f) 180 min. The inset in f depicts the interface between ZnO NRs and the substrate; the Ag thin film is completely dissolved.

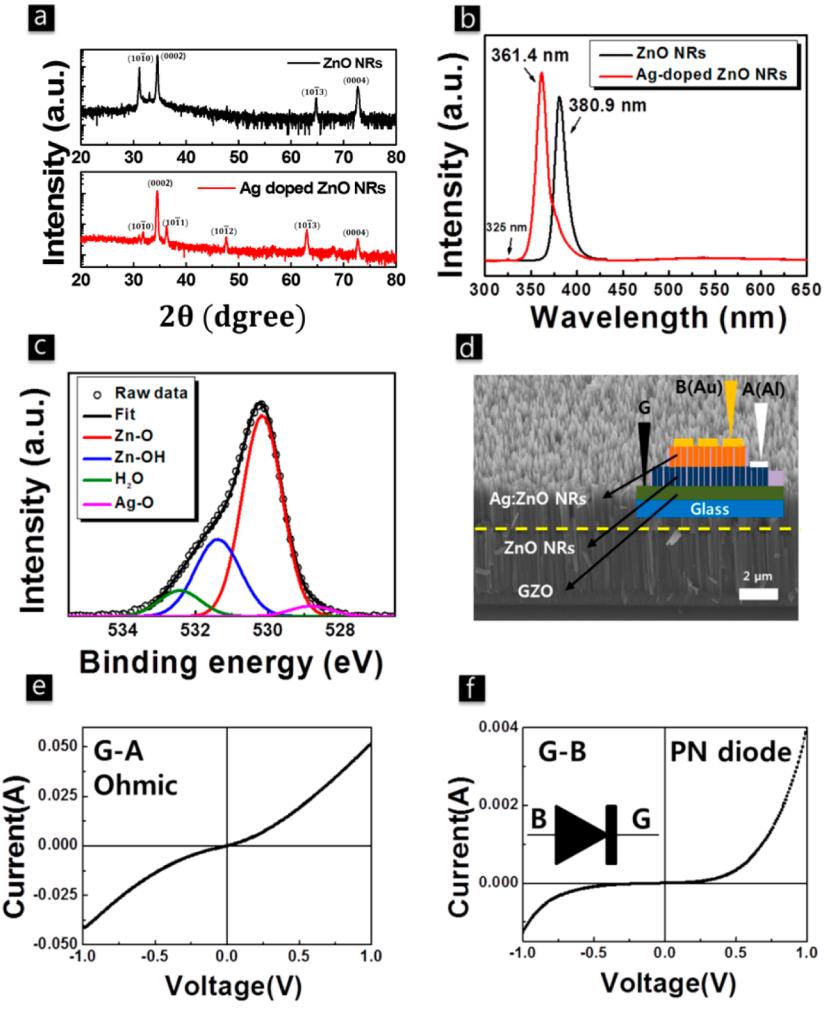


**Figure 2.** (a) XRD, (b) PL, and (c) XPS of Ag-doped and undoped ZnO NRs. (d) Cross-sectional SEM image of the p−n homojunction; the inset shows a schematic diagram of the p−n diode. (e) Ohmic *I*−*V* curve between the ground and active electrode A (G-A) and (f) p−n diode *I*−*V* curve between the ground and active electrode B (G-B).


dx.doi.org/10.1021/am504587x | *ACS Appl. Mater. Interfaces* 2014, 6, 15638−15642

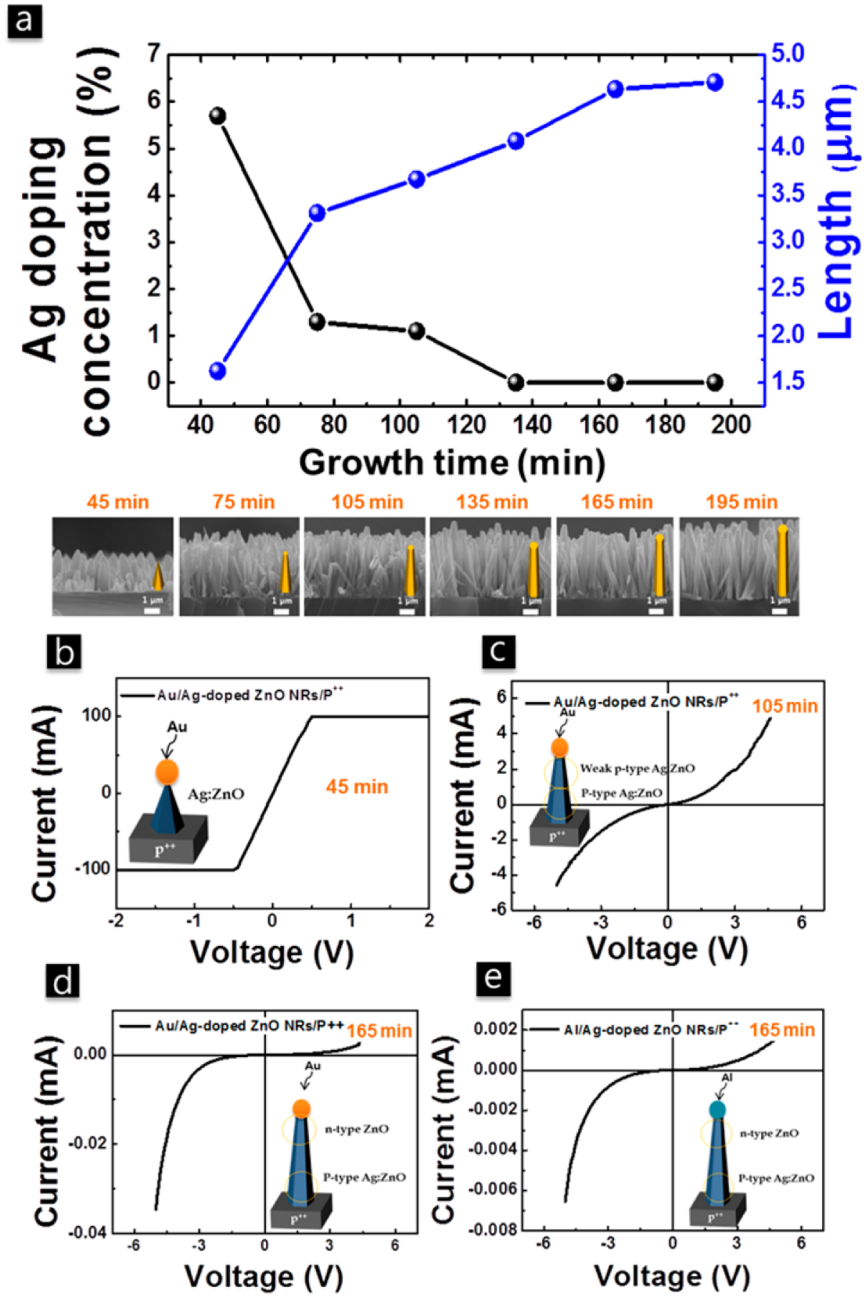


**Figure 3.** (a) Ag doping concentration and cross-sectional SEM image for each growth time. *I*−*V* characteristics for Ag-doped ZnO NRs on a heavily doped p-type Si wafer with a Au contact grown for (b) 45, (c) 105, (d) 165, and (e) Ag-doped ZnO NRs on a heavily doped p-type Si wafer with an Al contact grown for 165 min.

homojunction of ZnO NRs. The growth features of ZnO NRs on a Ag film varying with hydrothermal reaction time were experimentally determined and the results are shown in Figures 1(b)−(f). The four steps in dissolving Ag and growing ZnO NRs were clearly observed and confirmed. At 180 min, the Ag film was completely dissolved and ZnO NRs were densely grown on the substrate. The inset of Figure 1(f) shows that the Ag film between ZnO NRs and the substrate has completely disappeared. As an template without dissolving, a Au film was compared to the Ag film (see Figure S1). Unlike the Ag film, the Au film did not dissolve in the high pH conditions. Also, to determine the origin of the dissolution of the Ag film, a systematic experiment was conducted and the result is represented in Figure S2. The main chemical dissolving Ag was ammonium hydroxide ($NH_4OH$). By taking advantage of the selective growth of ZnO NRs on the (111) plane of the Ag crystal, various growth features were obtained using shaped Ag crystals as the template and the results are demonstrated in Figure S3.

Figure 1 (a) Four steps describing the growth of ZnO NRs on a Ag template. Temporal growth of ZnO NRs on a Ag thin film after (b) 30 min, (c) 45 min, (d) 60 min, (e) 75 min, and (f) 180 min. The inset in (f) depicts the interface between ZnO NRs and the substrate; the Ag thin film is completely dissolved.

The doping of Ag atoms into the ZnO NRs was confirmed through X-ray diffraction (XRD), photoluminescence (PL), and X-ray photoelectron spectroscopy (XPS) as shown in Figures 2(a)−(c), respectively. In the XRD pattern shown in Figure

2(a), the (0002) peak of the Ag-doped ZnO NRs was shifted to a lower angle compared with that of undoped ZnO NRs. Based on this shift, it was determined that the interplanar distance of (0002) expanded from 2.5937 to 2.6085 nm upon Ag doping. The increase in the *c*-axis lattice constant was caused by the larger ionic radius of the $Ag^+$ ion compared with the $Zn^{2+}$ ion. This structural expansion was also represented by the shifting of the $(10\bar{1}0)$ peak as shown Figure 2(a). Figure 2(b) shows the PL spectra of undoped and Ag-doped ZnO NRs. The band edge peak of Ag-doped ZnO NRs was shifted to lower wavelengths and the intensity increased compared with that of the undoped NRs. These results are in agreement with Pavesi's report[11] that the intensity of the band edge peak strongly depends on the doping concentration of $Ag^+$ ions into the ZnO lattice and that the peak position shows a blue shift upon increasing the doping concentration due to a decrease in the average distance between the donor and acceptor. For quantitative evidence of Ag doping, XPS was used to analyze the O 1s peak from the Ag-doped ZnO NRs, as shown in Figure 2(c). We identified the O 1s peak by the defect fitting and coupling of ZnO, Zn−OH bonds, adsorbed oxygen species, and Ag−O bonds. The quantitative atomic fractions of the present bonds were 50.3%, 22.3%, 26.3%, and 1.2%, respectively. The existence of Ag−O bond represents that the $Ag^+$ ions are actually doped into the ZnO crystal structure.

Figure 2 (a) XRD, (b) PL, and (c) XPS of Ag-doped and undoped ZnO NRs. (d) Cross-sectional SEM image of the p−n homojunction; the inset shows a schematic diagram of the p−n diode. (e) Ohmic I−V curve between the ground and active electrode A (G-A) and (f) p−n diode I−V curve between the ground and active electrode B (G-B).

To determine the electronic properties of the Ag-doped ZnO NRs, a device (Au/Ag-doped ZnO NRs/undoped ZnO NRs/Ga-doped ZnO (GZO) film) was fabricated as shown in the inset of Figure 2(d). First, undoped n-type ZnO NRs were grown on the GZO film, which acts as a bottom electrode. Then, a 50 nm-thick Ag thin film was deposited on the n-type ZnO NRs and Ag-doped ZnO NRs were grown for 150 min. The voids between the NRs were filled with poly(methyl methacrylate) (PMMA). The device was completed by depositing a Au thin film as a top electrode. Additionally, to determine the properties of the undoped ZnO NRs and GZO junction, Al was deposited on the undoped ZnO NRs grown on a GZO film. As shown in Figure 2(d), the Ag-doped ZnO NRs were successfully stacked on the undoped ZnO NRs grown on the GZO film. A ground (G) probe was connected to the GZO film and the active probes A and B were connected to the Al and Au electrodes, respectively. In the G-A probe combination, a typical I−V curve showing Ohmic contact was measured, as shown in Figure 2(e). On the other hand, the G-B probe combination displayed an I−V curve characteristic of a p−n junction, as shown in Figure 2(f). As a result, it was confirmed that the Ag-doped ZnO NRs have p-type semiconducting properties. The concentration of $Ag^+$ ions in the hydrothermal solution decreases with the time due to the finite thickness of the Ag film as a temporal dopant source. This result produces a gradient in Ag-doping concentration along the longitudinal direction of the ZnO NRs. To determine the Ag doping concentration with growth time, the atomic percent of Ag−O near the surface of ZnO NRs was measured at every 30 min from 45 to 195 min. For each case, XPS analysis was carried out and the results are shown in Figure S4. Between 45 and 75 min, the doping concentration dramatically decreased as shown in Figure 3, which represents that the 50 nm-thick Ag film was almost completely dissolved within 75 min. After the abrupt consumption of the Ag source, about 1 at% of Ag was incorporated into the ZnO NRs. Based on the data in Figure 3, we observed that the Ag film completely disappeared after 135 min, after which the ZnO NRs were continuously grown without Ag doping to form an n-type semiconductor. As the growth time increases, the length of the NRs increase and saturates due to the depletion of Zn ions in solution. As a result, a p−n homojunction of ZnO NRs was naturally formed during this simple hydrothermal process using a Ag template.

To investigate the characteristics of the p−n junction, electronic device configurations shown in Figures 3b−e were fabricated at different growth times and their *I*−*V* characteristics were measured. The Ag-doped ZnO NRs were grown on a heavily doped p-type silicon wafer ($p^{++}$ Si). For the ZnO NRs grown for 45 min, an *I*−*V* curve showing Ohmic contact was obtained from the Au/Ag-doped ZnO NRs/$p^{++}$ Si structure, implying that the Ag-doped ZnO NRs grown for 45 min have p-type semiconducting properties (Figure 3b). On the other hand, the ZnO NRs grown for 105 min show highly resistive Ohmic characteristic for the same device structure (Figure 3c).

In Figure 3a are shown the Ag doping concentration and cross-sectional SEM image for each growth time. *I*−*V* characteristics for Ag-doped ZnO NRs on a heavily doped p-type Si wafer with a Au contact grown for (b) 45 min, (c) 105 min, (d) 165 min, and (e) Ag-doped ZnO NRs on a heavily doped p-type Si wafer with an Al contact grown for 165 min.

The reason for this high resistance is that the carrier density inside the 105 min-grown ZnO NRs decreases due to the low Ag doping concentration. For the ZnO NRs grown for 165 min, a typical *I*−*V* curve showing a p−n junction was obtained from the Au/undoped n-type ZnO NRs/Ag-doped p-type ZnO NRs/$p^{++}$ Si structure (Figure 3d). On the basis of the *I*−*V* curve of Al/undoped n-type ZnO NRs/Ag-doped p-type ZnO NRs/$p^{++}$ Si shown in Figure 3e, it is concluded that the rectified *I*−*V* curve shown in Figure 3d originates not from the Schottky junction between Au and undoped n-type ZnO NRs but from the p−n homojunction between undoped n-type ZnO NRs and Ag-doped p-type ZnO NRs.

## CONCLUSIONS

In conclusion, a Ag thin film was introduced both as an template and a dopant source for vertically aligned p-type ZnO NRs. For the growth of ZnO NRs, ammonium hydroxide ($NH_4OH$) was used as a mineralizer under hydrothermal conditions. During the hydrothermal process, the Ag film was dissolved to generate $Ag^+$ ions in the reaction solution that were doped in the wurtzite structure of ZnO. The (111) plane of Ag also acted as a template for the (0001) plane of ZnO. Therefore, using this idea, Ag-doped p-type ZnO NRs were successfully grown on the substrate, which can be an electrode or n-type semiconductor for device applications. Ag doping was successfully verified through XRD, XPS, and PL analyses. The electronic p-type characteristics of Ag-doped ZnO NRs were demonstrated through the fabrication of p−n diodes. Upon depletion of the Ag and Zn sources, a gradient of Ag-doped ZnO NRs was fabricated and their *I*−*V* characteristics were determined.

## ■ ASSOCIATED CONTENT

### Supporting Information

Experimental methods, ZnO NRs grown with a Au film, investigation into Ag film dissolution, Ag-doped ZnO NR growth features using different shaped templates, and O 1s XPS spectra. "This material is available free of charge via the Internet at http://pubs.acs.org."

## ■ AUTHOR INFORMATION

### Corresponding Author

*E-mail: jmmyoung@yonsei.ac.kr.

### Author Contributions

†J.H. Park and T.I. Lee contributed equally to the work and share cofirst authorship.

### Notes

The authors declare no competing financial interest.

## ■ ACKNOWLEDGMENTS

This research was supported by WCU program through the National Research Foundation of Korea funded by the Ministry of Education, Science and Technology [*R*32-20031] and by the LG Display academic industrial cooperation program.

## ■ REFERENCES

(1) Baruah, S.; Dutta, J. Hydrothermal growth of ZnO nanostructures. *Sci. Technol. Adv. Mater.* **2009**, *10*, 013001−013018.

(2) Fang, X.; Li, J.; Zhao, D.; Shen, D.; Li, B.; Wang, X. Phosphorus-Doped p-Type ZnO Nanorods and ZnO Nanorod p−n Homojunction LED Fabricated by Hydrothermal Method. *J. Phys. Chem. C* **2009**, *113*, 21208−21212.

(3) Chang, H.; Sun, H.; Ho, K.; Tao, X.; Yan, F.; Kwok, W.-M.; Zheng, Z. A highly sensitive ultraviolet sensor based on a facile in situ solution-grown ZnO nanorod/graphene heterostructure. *Nanoscale* **2011**, *3*, 258−264.

(4) Wang, J. X.; Sun, X. W.; Yang, Y.; Huang, H.; Lee, Y. C.; Tan, O. K.; Vayssieres, L. Hydrothermally grown oriented ZnO nanorod arrays for gas sensing applications. *Nanotechnology* **2006**, *17*, 4995−4998.

(5) Wang, Z. L.; Song, J. Piezoelectric Nanogenerators Based on Zinc Oxide Nanowire Arrays. *Science* **2006**, *312*, 242−246.

(6) Shin, B.-K.; Lee, T.-I.; Xiong, J.; Hwang, C.; Noh, G.; Cho, J.-H.; Myoung, J.-M. Bottom-up grown ZnO Nanorods for an antireflective moth-eye structure onCuInGaSe2 solar cells. *Sol. Energy Mater. Sol. Cells* **2011**, *95*, 2650−2654.

(7) Wei, Y.; Ke, L.; Kong, J.; Liu, H.; Jiao, Z.; Lu, X.; Du, H.; Sun, X. W. Enhanced photoelectrochemical water-splitting effect with a bent ZnO nanorod photoanode decorated with Ag nanoparticles. *Nanotechnology* **2012**, *23*, 235401−235408.

(8) Xu, S.; Adiga, N.; Ba, S.; Dasgupta, T.; Wu, C.; Wang, Z. L. Optimizing and Improving the Growth Quality of ZnO Nanowire Arrays Guided by Statistical Design of Experiments. *ACS Nano* **2009**, *3*, 1803−1812.

(9) Lee, T.; Lee, S. H.; Kim, Y.-D.; Jang, W. S.; Oh, J. Y.; Baik, H. K.; Stampfl, C.; Soon, A.; Myoung, J. M. Playing with Dimensions: Rational Design for Heteroepitaxial p−n Junctions. *Nano Lett.* **2012**, *12*, 68−76.

(10) Fabrega, J.; Fawcett, S. R.; Renshaw, J. C.; Lead, J. R. Environ. Silver Nanoparticle Impact on Bacterial Growth: Effect of pH, Concentration, and Organic Matter. *Sci. Technol.* **2009**, *43*, 7285−7290.

(11) Pavesi, L.; Guzzi, M. Photoluminescence of AlxGa1−xAs alloys. *J. Appl. Phys.* **1994**, *75*, 4779−4842.